Electronic Supplementary Material (ESI) for Journal of Materials Chemistry A.

Unraveling the Li^+ desorption behavior and mechanism of $Li_4Ti_5O_{12}$ with different facets to enhance lithium extraction

Bing Zhao[a, b], Yingjun Qiao[a], Zhiqiang Qian[a], Wenfei Wei*[a], Jun Li[a], Zhijian Wu[a] and Zhong Liu*[a]

[a] Key Laboratory of Comprehensive and Highly Efficient Utilization of Salt Lake Resources, Qinghai Provincial Key Laboratory of Resources and Chemistry of Salt Lakes, Qinghai Institute of Salt Lakes, Chinese Academy of Sciences, Xining, Qinghai 810008, China

[b] University of Chinese Academy of Sciences, Beijing 100049, China

*Corresponding author, E-mail address: weiwf@isl.ac.cn; liuzhong@isl.ac.cn

1 Experiments and calculation methods

1.1 Data processing

The adsorption and desorption properties were evaluated by adsorption capacity (q_e), desorption efficiency (∂), distribution coefficient (K_d), and separation factor (a_{Me}^{Li}), respectively. They were calculated using the following equations:

$$q_e = \frac{(C_0 - C_e)V_1}{m} \quad (1)$$

$$\partial = \frac{C_t V_2}{s} \quad (2)$$

$$K_d = \frac{(C_0 - C_e)*1000*V_1}{C_e*m_1} \quad (3)$$

$$a_{Me}^{Li} = \frac{K_d(Li)}{K_d(Me)} \quad (Me = Na, K. Rb, Cs) \quad (4)$$

where C_0 and C_e (mg/L) are the initial and equilibrium concentrations of Li^+; C_t (mg/L) represents the concentration of Li^+ at some times; V_1 and V_2 (L) are the volumes of the LiCl solution and the desorption solution; m (g) and s (mg) denote the amounts of the adsorbent and Li^+/Ti^{4+} in the adsorbent, respectively.

1.2 Model fitting

The dates of adsorption isotherms were fitted by the Langmuir, Freundlich models and these equations can be depicted in Eq. (5) and Eq. (6).

Langmuir model: $\frac{C_e}{q_e} = \frac{1}{q_m b} + \frac{C_e}{q_m}$ (5)

Freundlich model: $lnq_e = lnK_F + \frac{1}{n} lnC_e$ (6)

where C_e is the equilibrium concentration (mg/L). b is the adsorption intensity or Langmuir coefficient related to the affinity of the binding site (L/mg). K_F and $1/n$ are the constants that are related to the adsorption capacity and the adsorption intensity, respectively.

Meanwhile, the Li^+ adsorption activities on HTO-s were explained by the pseudo-first-order (Eq. (7)) and pseudo-second-order (Eq. (8)) models, these equations were written as:

Pseudo-first-order: $q_t = q_e(1 - e^{-K_1 t})$ (7)

Pseudo-second-order: $q_t = \frac{K_2 q_e^2 t}{1+K_2 q_e t}$ (8)

Intra-particular diffusion model: $q_t = K_{dif} t^{0.5} + C$ (9)

where q_e and q_t (mg/g) are the amounts of cesium ions absorbed at equilibrium and at time t; and K_1 (min^{-1}) and K_2 (g/mg/min) denote the pseudo-first-order and pseudo-second-order constants. K_{dif} is the intra-particular diffusion rate constant ($mg/g/min^{1/2}$).

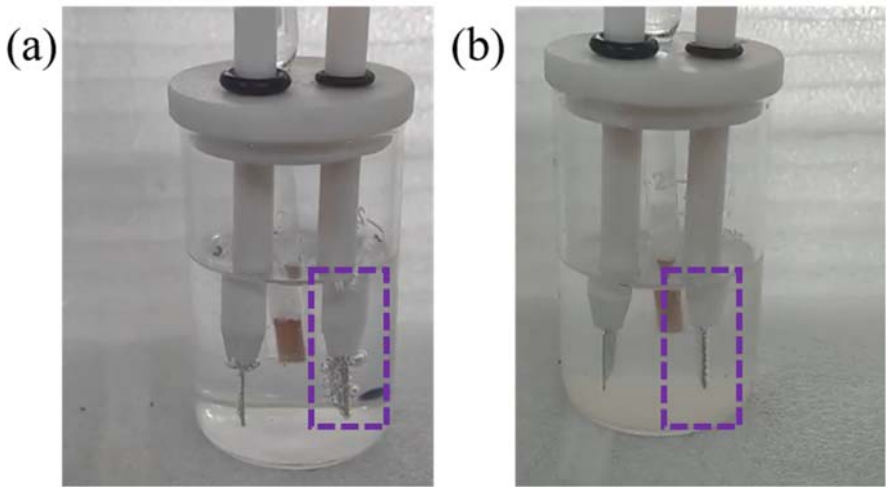

Fig. S1. The pictures of different solutions recorded during the LSV process: (c) before desorption (pure HCl sloutions) and after desorption (desorption time: 24 h).

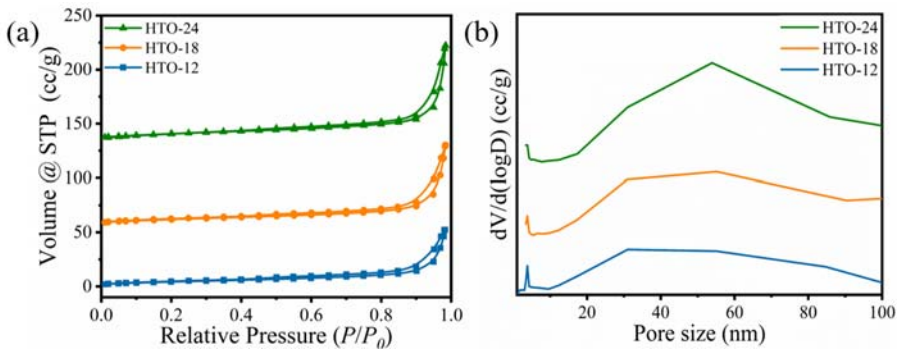

Fig. S2. The (a) N_2 ad-desorption isotherms and (b)pore distributions of HTO-s.

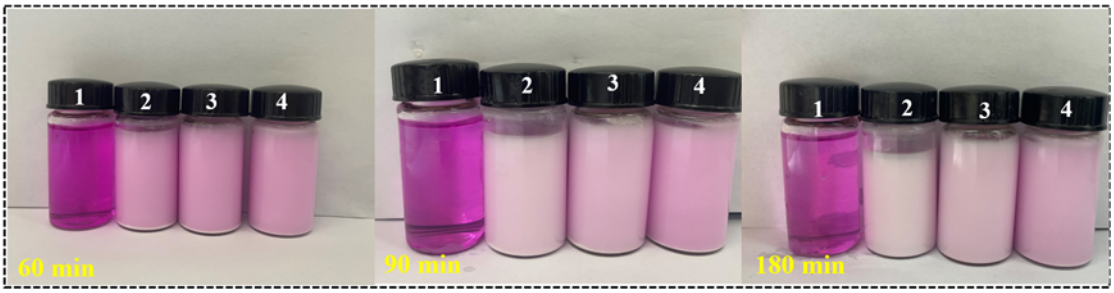

Fig. S3. Visualization adsorption experiments with adding different adsorbents (1: without absorbent, 2: HTO-12, 3: HTO-18, 4: HTO-24) with different adsorption times.

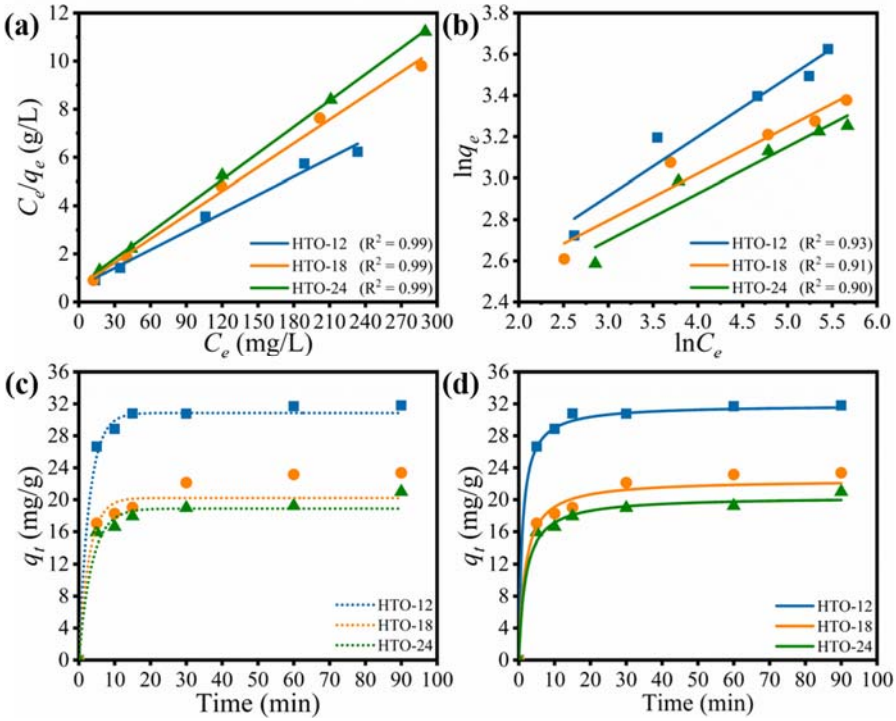

Fig. S4. The adsorption curves were fitted by different models: (a) Langmuir, (b) Freundlich, (c) pseudo-first-order and (d) pseudo-second-order models.

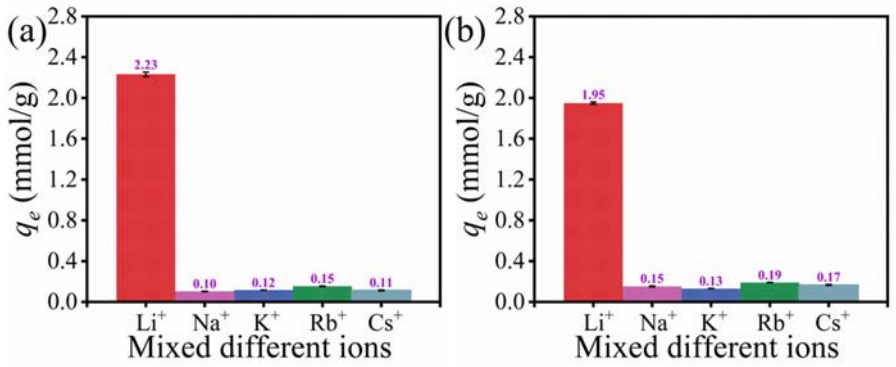

Fig. S5. The adsorption selectivity of Li^+ by HTO-s: (a) HTO-18 and (b) HTO-24.

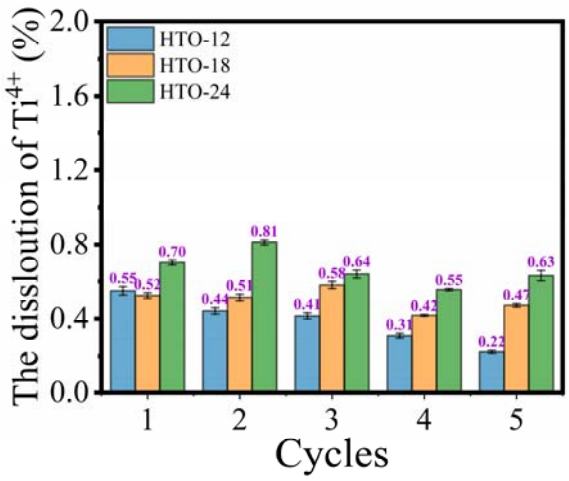

Fig. S6. The dissolution loss of Ti^{4+} in each cycle by HTO-s.

Table S1. The Intra-particular diffusion fitting parameters of Li^+ extraction during the desorption process.

T	Intra-particular diffusion					
	K_1 (mg/g·min$^{0.5}$)	R^2	K_2 (mg/g·min$^{0.5}$)	R^2	K_3 (mg/g·min$^{0.5}$)	R^2
HTO-12	1.44	0.96	0.28	0.64	0.03	0.91
HTO-18	0.95	0.98	0.51	0.95	0.01	0.47
HTO-24	1.34	0.99	0.93	0.70	0.03	0.75

Table S2. The Intra-particular diffusion model fitting parameters of Ti^{4+} dissolution during the desorption process.

T	Intra-particular diffusion			
	K_1 (mg/g·min$^{0.5}$)	R^2	K_2 (mg/g·min$^{0.5}$)	R^2
HTO-12	1.54	0.99	0.35	1.00
HTO-18	1.06	0.97	0.67	1.00
HTO-24	0.91	0.97	0.75	1.00

Table S3. The Langmuir and Freundlich models fitting parameters of HTO-s towards Li^+ adsorption.

T	Langmuir model			Freundlich model		
	q_m (mg/g)	*b* (L/mg)	R^2	K_F ((mg/g)(L/mg)1/n)	1/n	R^2
HTO-12	39.54	60.86	0.99	7.81	0.29	0.93
HTO-18	30.32	47.10	0.99	8.32	0.23	0.91
HTO-24	27.44	38.96	0.99	7.56	0.23	0.90

Table S4. The Intra-particular diffusion fitting parameters of HTO-s towards Li^+ adsorption in 249.88 mg/L LiCl solutions at 45°C.

T	Intra-particular diffusion					
	K_1 ($mg/g \cdot min^{0.5}$)	R^2	K_2 ($mg/g \cdot min^{0.5}$)	R^2	K_3 ($mg/g \cdot min^{0.5}$)	R^2
HTO-12	2.55	0.99	0.27	0.93	0.01	1.00
HTO-18	1.26	0.99	0.65	0.85	0.04	1.00
HTO-24	1.20	0.86	0.50	0.97	0.02	1.00

Table S5. The fitting parameters of adsorption kinetics by Pseudo-first-order and Pseudo-second-order models.

249.88 mg/L LiCl	Pseudo-first-order				Pseudo-second-order		
	$q_{e,exp}$ (mg/g)	$q_{e,cal}$ (mg/g)	K_1	R^2	$q_{e,cal}$ (g/mg/min)	K_2	R^2
HTO-12	31.80	30.86	0.35	0.93	31.88	0.03	0.90
HTO-18	23.37	20.22	0.35	0.50	22.50	0.02	0.83
HTO-24	20.99	18.88	0.27	0.56	20.38	0.03	0.87

Table S6. Adsorption selectivity by HTO-s in solutions containing Li^+, Na^+, K^+, Rb^+, Cs^+.

Metal ions	HTO-12			HTO-18			HTO-24		
	q_e (mmol/g)	K_d (mL/g)	a_M^{Li}	q_e (mmol/g)	K_d (mL/g)	a_M^{Li}	q_e (mmol/g)	K_d (mL/g)	a_M^{Li}
Li^+	3.06	729.04	1.00	2.23	484.48	1.00	1.95	410.49	1.00
Na^+	0.11	27.86	26.16	0.10	26.49	18.29	0.15	39.21	10.47
K^+	0.12	7.90	92.29	0.12	7.83	61.88	0.13	8.61	47.70
Rb^+	0.15	16.18	45.06	0.15	16.77	28.88	0.19	20.65	19.87
Cs^+	0.09	22.35	32.63	0.11	27.16	17.84	0.17	41.50	9.89